Dynamics of water in the amphiphilic pore of amyloid β fibrils ☆

CrossMark

Pavan K. GhattyVenkataKrishna [a,*], Barmak Mostofian [b]

[a] Computational Biology and Bioinformatics Group and BioEnergy Science Center, Oak Ridge National Laboratory, Oak Ridge, TN 37831, USA
[b] UT/ORNL Center for Molecular Biophysics, Oak Ridge National Laboratory, Oak Ridge, TN 37831, USA

ARTICLE INFO

Article history:
Available online 19 July 2013

ABSTRACT

Alzheimers disease related amyloid peptide, Aβ, forms a fibrillar structure through aggregation. The aggregate is stabilized by a salt bridge that is responsible for the formation of an amphiphilic pore that can accommodate water molecules. None of the reported structures of Aβ, however, contain water. We present results from molecular dynamics simulations on dimeric Aβ fibrils solvated in water. Water penetrates and fills the amphiphilic pore increasing its volume. We observe a thick wire of water that is translationally and rotationally stiff in comparison to bulk water and may be essential for the stabilization of the amyloid Aβ protein.

© 2013 The Authors. Published by Elsevier B.V. All rights reserved.

1. Introduction

Water is the scaffold which supports all known life. Water allows diverse and complex life forms to exist, flourish and evolve. It is a crucial matrix which supports all the important steps for successful survival of an organism; transcription, translation and replication. It affects how DNA folds/unfolds, is transcribed, translated into proteins and how proteins maintain/lose their structure and function. The folding of proteins in water is a widely investigated field with important implications [1,2]. Water not only helps with the folding of proteins but is an integral component of the protein's structure in many cases [3–6]. Further, a critical amount of water known as hydration water is required to activate the function of some proteins [7–11]. Although bound water helps stabilize some proteins, capturing the structural details of that water to the same degree as that of the host protein is difficult. This is due to the relatively high mobility coupled with the small size of water molecules. In addition to this, some experimental techniques lack the resolution required to capture this detail. The problem is compounded when the host protein cannot be crystallized as is the case in the β sheets formed by Alzheimer's related amyloid peptides.

Amyloid peptides in Alzheimer's afflicted human brains are formed due to the proteolytic cleavage of the larger amyloid precursor protein (APP); first by β secretase and then by γ secretase [12]. This results in the formation of a 40/42 amino acid peptide which has the following sequence $D_1AEFRHDSGY_{10}$ $EVHHQKL_{17-}VFF_{20}$ $AEDVGSNKGA_{30}$ $IIGLMVGGVV_{40}IA_{42}$ and will henceforth be referred to as the amyloid peptide. The amyloid peptide folds into a hairpin structure in which the arms of the hairpin form β sheets with the same arm of another amyloid peptide resulting in an in-register β sheet. These sheets extend into extremely long fibrils, supra-fibrils and other higher order structures which have been observed in diseased brains. The two arms of the hairpin are connected by a loop region whose exact length and constituent amino acids is currently under debate. Regardless, there exists a consensus in the debate that there is a strong salt bridge between D23 and K28 which is necessary for the formation and stabilization of the β sheets. In fact, fibril formation is affected when the salt bridge was disrupted[13]. Some anti-amyloid drugs have been argued to function by destabilizing the salt bridge [14]. Also loop forming tendency of residues 22–28 (that include the D23–K28 salt bridge) has been shown to be independent of degree of aggregation [15]. Due to this salt bridge and due to the above-plane and below-plane arrangement (where plane refers to the β sheet) of side chains of adjacent amino acids, an amphiphilic nanopore is formed by amyloid peptide aggregates. Multiple computational studies [16–18] point to the wetting of this nanopore. However, none of the structures of amyloid β sheets submitted to Protein Data Bank contain water which is due to the limitation of the experimental techniques used to determine the structures: ssNMR [19] and cryo-EM [20]. Thus details of the structure and dynamics of these β sheets are incomplete without a discussion on the water molecules wetting the amphiphilic cavity. Although many pioneering studies have directed their attention towards the host protein, far fewer studies have a rigorous discussion of the embedded water molecules.

Zheng et al. studied the pore formed by 5 amyloid chains stacked axially in both monomeric (single hairpin per cross-section) or dimeric (double hairpin per cross-section) fibrils and found

---

* Corresponding author.
E-mail addresses: pkc@ornl.gov, pavanghatty@gmail.com (P.K. GhattyVenkataKrishna).

its average size to be between 7 and 8 Å and the embedded water molecules to be slower than bulk water [16]. Thirumalai and co-workers found that water molecules prevent the formation of D23–K28 salt bridge when the protein exists in a dilute solution as a single peptide [21]. In an extended review by the same group, the stability of the salt bridge in a mature fibril is argued as being mediated by the pore-hydrating water [17]. Both Buchete et al. [18] and Lemkul & Bevan [22] found the salt bridge to be necessary for the fibril stability.

Dynamics of water under confinement is an extremely rich and interesting field of research. Thin water wires formed in hydrophobic [23–26] and hydrophilic spaces [23] have been studied. Water movement in these tight spaces in the presence and absence of external electric fields have also been studied [27–29]. Movement of water through aquaporins has received wide attention in the past decade due to the increased availability of structures of relevant transmembrane proteins [30–32]. While the results of these studies offer important guidance, they are not directly applicable in the case of amyloid β sheet nanopores due to two reasons: (a) there is no evidence that water moves through this nanopore in any particular direction, therefore this water can be thought of as an extension of the protein's structure rather than a fleeting entity and (b) due to the presence of the salt bridge on one side of the pore's cross-section and hydrophobic residues on the other side, the pore is amphiphilic and this sets it apart as a special and interesting case.

In this communication we report results from molecular dynamics simulations and address important details on the translational, rotational and hydrogen bonding properties of water molecules trapped in the amphiphilic nanopore created by amyloid β sheets. We show that a dry pore swells to three times its volume to accommodate water molecules and upon stabilization, the density inside the pore is comparable to bulk values.

2. Results and discussion

2.1. Penetration of the amyloid pore by water

The focus of this work is on pore water and its properties. Therefore, an accurate definition of the pore is necessary. In this study, a pore is formed by the axial stacking of 20 amyloid chains. Water molecules spanning the length of first 5 chains on each end are not considered for analysis. This is done to avoid artifacts caused by end chains which are more flexible and therefore less stable than the central 10 chains. Therefore from here onwards only the water molecules filling the central 10 chains of a 20 chain long fibril are considered for analysis. Water enters the amyloid nanopore from both ends in our simulations (refer to Figure 1a). The central 10 chains can, on average, accommodate 56 water molecules as can be seen in Figure 2. As water fills the central 10 chains, the density fluctuates around the bulk value of 1gm/cc before stabilizing at the near bulk value of 1.11 ± 0.03 g/cc.

Since water molecules approach from both sides of the pore, we do not observe a net flow of solvent into any one direction along the pore axis as in other studies on water conduction through nanopores [26,28]. Instead, upon reaching a steady number of 56 in the central section, exchange between pore waters from this section and those from the two pore ends is reduced and most water molecules remain in the pore center for the remainder of any simulation. For the analysis of pore water structure and dynamics, we considered the last nanosecond of each simulation and we took into account only those water molecules that remain in the pore's central section for more than 70% of that time. On average, 47 water molecules fit this definition which indicates the relatively low migration of pore waters.
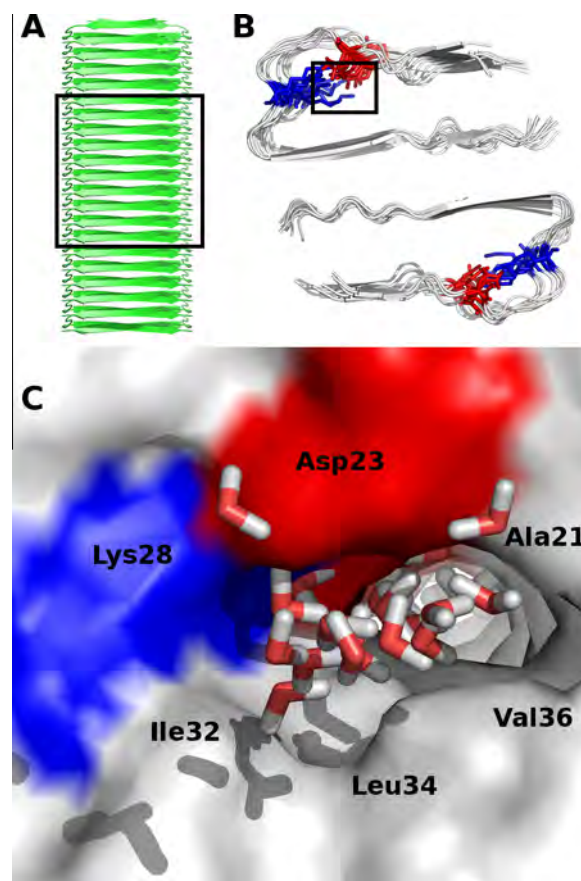
Figure 1. (A) Top view of the fibril formed by 20 peptides. The black rectangle highlights the central region considered for analysis in this study. (B) Axial view of the fibril showing a dimer. (C) Close-up of a hydrated pore formed by the D23–K28 salt bridge. Corresponds to the box highlighted in B. Protein residues responsible for the formation of the pore. Notice the polar residues Asp23 and Lys28 on one side of the pore wall and hydrophobic residues Ala21, Ile32, Leu34 and Val36 on the other side of the pore wall.

Due to the flexibility of the β sheets, the pore volume increases upon water penetration (Figure 2) and reaches a steady value towards the end of the simulation which is 3 times that of the 'dry' state. Hence, our findings describe a scenario where the Aβ fibril swells to increase its pore size and accommodate enough water so that the density inside the pore equals that of bulk. It should be mentioned that although the amyloid structure allows an increase in pore volume, the pore's cylindrical structure remains intact during all simulations. The volume change as well as the amphiphilic interior are characteristic features of the amyloid nanopore making it an interesting environment in which to study the structure and dynamics of water molecules.

2.2. Pore water structure

The first peak of the intermolecular radial distribution function of pore water molecules is at the same value as those of bulk water, that is at 2.8 Å for oxygen–oxygen and at 1.8 Å for oxygen–hydrogen interactions (data not shown). Therefore the interatomic distances are the same in pore and bulk water. This is not surprising since unlike other cases of water under confinement, water in Aβ pore is in the form of a thick wire and not in a single file along the pore axis. This water wire is defined by intermolecular hydrogen bonds to which the above-mentioned RDF peak values correspond. When confined inside the pore, however, water molecules cannot form hydrogen bonds with as many surrounding water molecules as in bulk. We calculated the hydrogen bonds using a geometric criteria.
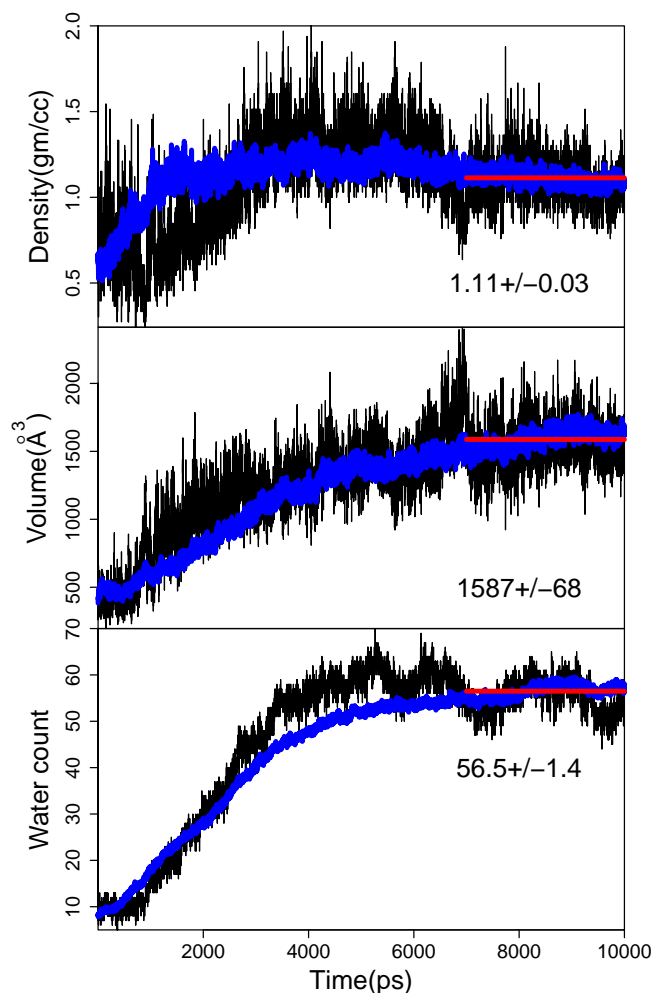
Figure 2. Density, volume and number of water molecules in the pore as a function of simulation time. Data from 1 of the 20 pores studied is shown in black. The blue line is the averaged data from all the 20 pores where each pore is formed by 10 amyloid peptides and is approximately 45 Å long. The red line shows the mean of the last 3 ns of the averaged data. This mean and standard deviation are displayed on the plot. (For interpretation of the references to color in this figure legend, the reader is referred to the web version of this article.)

A hydrogen bond was supposed to form when the distance between the donor and acceptor oxygens was 3.5 Å and the O–H···O angle was more than 150°. Interestingly, the total number of hydrogen bonds a pore water can make (as either acceptor or donor) is 2.5 and thus comparable to the corresponding bulk value (Figure 3). A similar observation regarding bulk and pore water was made in another study involving water in amphiphilic pores [33]. Nevertheless, only around one third of all hydrogen bonds formed by a pore water are with other pore waters while the remaining two thirds are made with protein residues. On average, about half of the hydrogen bonds involving protein atoms are with the charged amino acids D23 and K28, which are crucial for pore formation and which contribute to its amphiphilicity. This shows that the amyloid pore surface helps maintain the average number of hydrogen bonds per water molecule in confinement. Moreover, the charged residues on the pore surface clearly play a major role in binding water. Additionally, the hydrogen bonding properties of pore and bulk water were calculated using methods described in Ref. [34]. As shown in supporting material (Figure S1), the hydrogen bond network relaxation time of water molecules inside the pore is slightly increased compared to bulk water hydrogen bonds. This implies longer existing hydrogen bonds which dampen the dynamics of the pore water molecules.
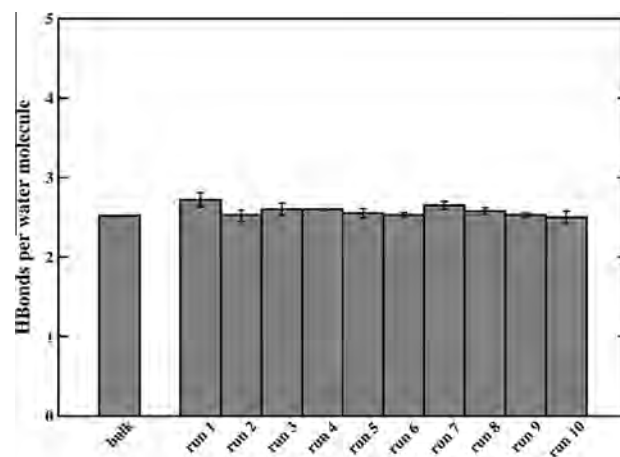
Figure 3. Average number of hydrogen bonds formed by bulk and pore water molecules. 66% of the hydrogen bonds made by pore waters are with protein residues while the remainder are with other pore waters. Data for each run is reported as the average of two pores.
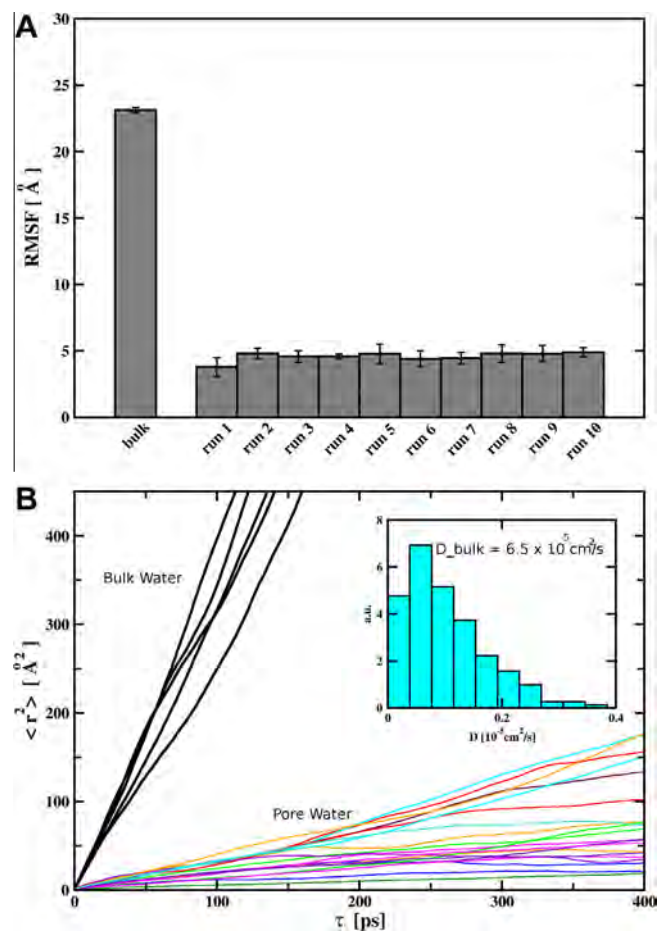
Figure 4. (A) RMSF of pore water molecules in each of the 10 runs compared to bulk water. Data for each run is reported as the average of two pores. (B) Mean squared displacement (MSD) of bulk and pore water molecules calculated during the last nanosecond of the simulation. The inset shows the distribution of diffusion coefficients derived from the slope of the MSD from pore water molecules.

2.3. Pore water dynamics

Visual inspection of the simulation trajectories revealed that pore water molecules moved slower than bulk water molecules.

Therefore, the fluctuation of water molecules around their mean position is calculated for the last nanosecond (Figure 4A). The histograms of average RMSFs show that these fluctuations are about five times lower in any amyloid nanopore ($\sim$5 Å) than in bulk water ($\sim$23 Å), which proves that pore water molecules are restrained in their motion. The diffusion coefficient calculated from the mean squared displacement of pore water also clearly shows reduced motion compared to bulk water (Figure 4B). The self-diffusion coefficient, D, is on average between 0.1–0.2 $\times 10^{-5}$ cm^2/s which is comparable to previous studies on the diffusion of water in amyloid pores [16] while the corresponding value in bulk water is 6.5×10^{-5} cm^2/s. Thus, water is relatively stationary inside the pore.

Besides the reduced translational dynamics, pore waters also exhibit damped rotational dynamics. The dipole moment auto-correlation function, C_μ, was calculated as the quantity $\langle \boldsymbol{\mu}_{t+\Delta t} \cdot \mu_t \rangle$ where $\boldsymbol{\mu}$ is the unit vector along the dipole, Δt is the time window and angled brackets indicate moving time averages. The quantity C_μ varies between -1 to $+1$. This function for pore waters does not decay as it does for bulk water molecules where it becomes uncorrelated ($C_\mu = 0$) within 10 ps (see Figure S2). This means that water molecules inside the pore do not reorient as frequently as they do in bulk. Thus both the translational and rotational motion of pore water are damped compared to bulk water. Although water molecules confined in nanopores have been shown to have distinct orientation of the collective dipoles [24,29,28], pore waters in amyloid β sheets do not exhibit such behavior. This could be because of two reasons: (a) water molecules enter the pore from both directions and (b) unlike other studies there is not a single file of water molecules but rather a thick water wire is observed which was found to form as many hydrogen bonds as bulk water. Water has been previously shown to mediate and stabilize amyloid strands [35]. It is therefore possible that a thick wire formed by relatively immobile water found in this study contributes significantly towards stabilization of the amyloid hairpin dimers.

3. Conclusions

In summary, water has been found to fill the amphiphilic cavity formed in the loop region of amyloid β peptide. In this communication we address the static and dynamic properties of these pore water molecules and the pore itself. The pore expands to accommodate water molecules and equilibrium is reached when the water density in the pore equals the bulk value. Both the translational and rotational dynamics of the pore water are considerably damped in comparison to bulk water. Although the total number of hydrogen bonds made by bulk and pore water are comparable, 66% of hydrogen bonds made by pore waters are with the protein. Therefore at any given time, every pore water makes between one to two hydrogen bonds with protein atoms making it an important structural component of the protein. This underscores the importance of including pore water molecules while discussing structural and drug-design aspects of amyloid β sheets.

4. Methods and analysis

We used the central chain in model 10 PDB 2BEG (which was derived from cryo-EM) as the base unit for the hairpin. This hairpin was placed on an *x*–*y* plane and a 20mer was generated by placing new hairpins along the *z* axis with a 4.8 Å inter-peptide distance. This 20mer was rotated around the *z* axis by 180 to create a 40mer where M35 of the top 20mer interacts with M35 of the bottom 20mer to form a hydrophobic patch. This type of a dimer is generally referred to as C_{2z}. While other possible dimer structures have been proposed (Figure 3 in Ref. [36]), C_{2z} is considered most probable [37,16,19]. A 40mer prepared in this fashion has two pores one each in the top and bottom fibril. Each pore is approximately 95 Å long due to 19 inter chain distances of $\sim$5 Å (after equilibration). The 40mer was solvated with a 20 Å pad of water on all directions and 40 sodium ions were used to neutralize the system. The final simulation box has 65121 atoms of which 14960 are protein atoms, 40 are sodium ions and 50121 water atoms.

NAMD 2.9 [38] with CHARMM27 force field [39](with CMAP corrections [40]) for the protein and TIP3P model for water [41] was used for performing these calculations. All the simulations were performed in the NPT ensemble. Langevin thermostat with a damping coefficient γ of $1ps^{-1}$ was used for temperature control. Nosè–Hoover Langevin piston [42,43] with an oscillation period of 100 fs and damping time scale of 50 fs was used for pressure control. A time step of 2 fs was used during the entire length of the simulation. VMD [44] was used for data analysis, visualization and to generate pictures in both the main text and supporting material.

The first step in the simulation was a 10000 step steepest-descent minimization where the protein backbone atoms were restrained with a harmonic constraint of 5 kcal mol^{-1}Å^{-2}. After minimization, the temperature of the systems was set to 100 K and the harmonic restraints on the backbone were removed. The α carbon of residue M35 in chain 30, was fixed in all the simulations to arrest translation of the 40mer during the production run. After heating the systems from 100 K to 200 K in steps of 10 K/20 ps, 10 separate runs were conducted each with a different seed value to reinitialize velocities at 200 K. At this stage, the 10 runs were independently heated from 200 K to 310 K in steps of 10 K/20 ps. At 310 K all the runs were equilibrated for 1 ns after which 10 ns of data were collected. As described in the next sections, the last ns of the 10 ns was used for most of the analyses performed.

The bulk water simulation contained 13000 water molecules in a cubic box with a density of 1gm/cc. The simulation box was heated from 100 K to 310 K in steps of 10 K/20 ps after which 12 ns of data were collected – all in the NPT ensemble.

Volume of the pore was estimated by first calculating the solvent accessible surface area of the six protein residues defining the pore (A21, D23, L28, I32, L34 and V36) and equating it to the area of a hypothetical cylinder of length 45 Å(the distance between 10 amyloid chains with an inter-chain distance of 5 Å) and radius r. Using this approximation of radius the volume was calculated as $\pi r^2 45$ Å^3 for all the frames in the simulation.

Acknowledgments

Appendix A. Supplementary data

The supporting material contains two figures. The water–water hydrogen bond correlation function in bulk and in the pore and the decay of the dipole correlation function of water in bulk and in the pore. Supplementary data associated with this article can be found, in the online version, at http://dx.doi.org/10.1016/j.cplett.2013.07.026.

References

[1] Y. Levy, J.N. Onuchic, Annu. Rev. Biophys. Biomol. Struct. 35 (2006) 389.
[2] K.A. Dill, Biochemistry 29 (1990) 7133.
[3] X. Chen, I. Weber, R.W. Harrison, J. Phys. Chem. B 112 (2008) 12073.
[4] M. Levitt, B.H. (Park, Structure (London, England: 1993) 1 (1993) 223.
[5] J.L. Finney, Philos. Trans. R. Soc. B 278 (1977) 3.
[6] M. Frey, Acta Crystallogr. D 50 (1994) 663.
[7] J.A. Rupley, G. Careri, Adv. Protein Chem. 41 (1991) 37.
[8] M. Tarek, D.J. Tobias, Biophys. J. 79 (2000) 3244.
[9] A.L. Tournier, J. Xu, J.C. Smith, Biophys. J. 85 (2003) 1871.
[10] A.P. Sokolov, H. Grimm, R. Kahn, J. Chem. Phys. 110 (1999) 7053.
[11] B. Halle, Philos. Trans. R. Soc. B 359 (2004) 1207.
[12] A. Goate et al., Nature 349 (1991) 704.
[13] X. Yu, Q. Wang, J. Zheng, Biophys. J. 99 (2010) 666.
[14] T. Zhang, J. Zhang, P. Derreumaux, Y. Mu, J. Phys. Chem. B 117 (2013) 3993.
[15] Y. Chebaro, N. Mousseau, P. Derreumaux, J. Phys. Chem. B 113 (2009) 7668.
[16] J. Zheng, H. Jang, B. Ma, C.-J. Tsai, R. Nussinov, Biophys. J. 93 (2007) 3046.
[17] D. Thirumalai, G. Reddy, J.E. Straub, Acc. Chem. Res. 45 (2011) 83.
[18] N.-V.V. Buchete, R. Tycko, G. Hummer, J. Mol. Biol. 353 (2005) 804.
[19] A.T. Petkova, W.-M. Yau, R. Tycko, Biochemistry 45 (2005) 498.
[20] T. Lührs et al., Proc. Natl. Acad. Sci. U.S.A. 102 (2005) 17342.
[21] B. Tarus, J.E. Straub, D. Thirumalai, J. Am. Chem. Soc. 128 (2006) 16159.
[22] J.A. Lemkul, D.R. Bevan, J. Phys. Chem. B 114 (2010) 1652.
[23] T.W. Allen, S. Kuyucak, S.H. Chung, J. Chem. Phys. 111 (1999) 7985.
[24] R. Yang, T.A. Hilder, S.-H. Chung, A. Rendell, J. Phys. Chem. C 115 (2011) 17255.
[25] U.S. Raghavender, S. Aravinda, N. Shamala, R. Kantharaju Rai, P. Balaram, J. Am. Chem. Soc. 131 (2009) 15130.
[26] G. Hummer, J.C. Rasaiah, J.P. Noworyta, Nature 414 (2001) 188.
[27] J. Li, X. Gong, H. Lu, D. Li, H. Fang, R. Zhou, Proc. Natl. Acad. Sci. U.S.A. 104 (2007) 3687.
[28] J. Su, H. Guo, ACS Nano 5 (2010) 351.
[29] J. Su, H. Guo, J. Phys. Chem. B 116 (2012) 5925.
[30] E. Tajkhorshid, P. Nollert, M.Ø. Jensen, L.J.W. Miercke, J. O'Connell, R.M. Stroud, K. Schulten, Science 296 (2002) 525.
[31] K. Murata et al., Nature 407 (2000) 599.
[32] I. Johansson, M. Karlsson, V.K. Shukla, M.J. Chrispeels, C. Larsson, P. Kjellbom, Plant Cell Online 10 (1998) 451.
[33] V. Kocherbitov, J. Phys. Chem. C 112 (2008) 16893.
[34] A. Luzar, D. Chandler, Phys. Rev. Lett. 76 (1996) 928.
[35] S. Gnanakaran, R. Nussinov, A.E. García, J. Am. Chem. Soc. 128 (2006) 2158.
[36] B. Urbanc et al., Biophys. J. 87 (2004) 2310.
[37] N.L. Fawzi, Y. Okabe, E.-H. Yap, T. Head-Gordon, J. Mol. Biol. 365 (2007) 535.
[38] J.C. Phillips et al., J. Comput. Chem. 26 (2005) 1781.
[39] A.D. MacKerell et al., J. Phys. Chem. B 102 (1998) 3586.
[40] A.D. Mackerell, M. Feig, C.L. Brooks, J. Comput. Chem. 25 (2004) 1400.
[41] W.L. Jorgensen, J. Chandrasekhar, J.D. Madura, R.W. Impey, M.L. Klein, J. Chem. Phys. 79 (1983) 926.
[42] G.J. Martyna, D.J. Tobias, M.L. Klein, J. Chem. Phys. 101 (1994) 4177.
[43] S.E. Feller, Y. Zhang, R.W. Pastor, B.R. Brooks, J. Chem. Phys. 103 (1995) 4613.
[44] W. Humphrey, A. Dalke, K. Schulten, J. Mol. Graph. 14 (1996) 33.